Progress In Electromagnetics Research, PIER 33, 237–259, 2001

THE INFLUENCE OF THE FINITE SIZE OF THE ILLUMINATED AREA ON ELECTROMAGNETIC SCATTERING FROM SURFACES WITH AND WITHOUT SLICKS

A. I. Timchenko

Institute of Radiophysics and Electronics
National Academy of Sciences of Ukraine
12 Acad. Proskury St., 61085 Kharkov, Ukraine

A. E. Serebryannikov

Institute of Radio Astronomy
National Academy of Sciences of Ukraine
4 Chervonopraporna St., 61002 Kharkov, Ukraine

K. F. Schünemann

Arbeitsbereich Hochfrequenztechnik
Technische Universität Hamburg-Harburg
Denickestrasse 22, D-21073 Hamburg, Germany

Abstract—In this paper, the problem of scattering from sea surface with and without oil slicks is investigated taking the finite size of the illuminated area into account. A model of an inhomogeneous random rough surface with finite size of the scattering area is considered. To apply the results for a broad range of the random surface spectrum, an approach is developed which extends the range of validity beyond that of small perturbation theory. The general expression obtained for the scattering cross section takes into account a modulation of the rough surface by long surface waves. Analytical and numerical studies of the scattering cross section are provided to investigate the role of different mechanisms of scattering from various parts of the surface spectrum, and of diffraction caused by the finite size of the area. It is shown that the area size may affect the normalized scattering cross section in the case of the surface with a slick. Possibilities to explain the features of the suppression of the backscattering by oil slicks are discussed. Furthermore, a way to distinguish between different scattering mechanisms is suggested.

1 Introduction

2 Theory

3 Analysis

4 Simulation Results

5 Conclusions

References

1. INTRODUCTION

In recent years, the problem of oil slick identification from look-alike spots of SAR images has increasingly become important [1–5]. That task is, however, very complex particularly under low-wind conditions. To solve the problem it is necessary to develop an adequate model of electromagnetic wave scattering from sea surface with and without oil films.

During the past several decades, considerable efforts have been devoted towards the development of a theory for interpreting the backscattered signal from rough surfaces (see, for example, papers [6–9] and references given therein). To interpret the scattering from oil slicks and from the surrounding sea surface, one should use a model incorporating a broad range of the roughness spectrum. Despite of many attempts which have been done in this direction, models being developed by now do not describe the scattering process with sufficient accuracy. Another feature arising in the scattering problem is the finite size of the illuminated surface. This aspect should be taken into account for adequately interpreting oil slicks on SAR images.

The present study has been aimed on the development of a scattering model for a composite random rough surface with finite size of its illuminated area. The theoretical approach is based on a solution describing the scattering process from a random surface with moderate slopes.

In the general case, the sea surface may be inhomogeneous because of a modulation of the statistically homogeneous small-scale components by the large-scale part of the spectrum. This can correspond to swell or internal waves. Hence, the model to be developed should include a term being responsible for this effect. In the most interesting cases, the inhomogeneous part will be close to periodic or near-periodic, if it is caused by the joint effects of wind and gravity waves on capillary waves. In our model, the mean part of the modulating inhomogeneous part is described by a cosine function. Because the illuminated surface shows a finite size, ensemble averaging of the long wave contributions of the random surface is provided, while the small-scale roughness is averaged under the assumption of an infinitely wide illuminated area.

Numerical calculations have been carried out with the aid of this model, in a wide range of the variation of the roughness parameters which correspond to the surfaces with and without oil slicks. To apply the obtained results to the real experimental situation, the angular behaviour of the scattering cross section for different parameters of the rough surface is studied. The results of the study are discussed from the point of view of their usefulness to explain experimental data. In particular, the developed approach allows us to investigate the strong reduction of the surface roughness which appears when oil films are on sea surface.

2. THEORY

Consider scattering of a plane horizontally polarised electromagnetic wave from a perfectly conducting composite rough surface which may contain random parameters. A one-dimensional case is considered. We use here the integral-equation-based approach [10]. According to this approach, the scattered field in the far-field region is described by a Fredholm integral equation of the second kind. Solving the latter by using the perturbation technique approximation, one obtains the first term of the solution for the electric field as

$$E = \frac{-ik_z e^{-i\vec{k}\vec{R}_a}}{4\pi|\vec{R}_a|} \int_{-L}^{L} dx e^{i\chi_x x + i\chi_z \zeta(x)}. \tag{1}$$

Here $|\vec{R}_a|$ means distance between a point at the surface and the observation point, $\chi_x = |\vec{k}|(\sin\theta_i - \sin\theta_s)$, $\chi_z = |\vec{k}|(\cos\theta_i + \cos\theta_s)$, $k_z = |\vec{k}|\cos\theta_i$ where θ_i and θ_s are the incidence and scattering angles, respectively, $\vec{k}$ is the wave vector of the incident wave, and $\zeta(x)$ means height roughness as a function of the horizontal coordinate x.

The scattering cross-section is expressed as

$$\sigma \sim \int_{-L}^{L}\int_{-L}^{L} dx dx' e^{i\chi_x(x-x') + i\chi_z[\zeta(x)-\zeta(x')]}. \tag{2}$$

Note that (1) has been applied by many authors under the assumption that the size of the illuminated area is much larger than any peculiar linear scale of a random component of the surface (e.g., the correlation length), which is introduced by averaging. (See, for example, [7, 9, 11]). However, this assumption is not always satisfied in a realistic experimental situation. Hence we will carry out the integration over an area whose linear size is $2L$, without averaging in the integrand of (2) with respect to those parameters of the surface components whose individual scale is large compared to the electromagnetic wavelength λ. The random nature of the above component will further be taken into account by ensemble averaging.

Consider the case of a composite two-component surface which is given by

$$\zeta(x) = A\cos(Kx + \phi) + \zeta_1(x). \tag{3}$$

Here A and K are, respectively, amplitude and wave number of the periodical surface component, ϕ is phase of the periodical component, and $\zeta_1(x)$ means height of the small-scale roughness. It can be assumed that $Ak \gg 1$ where k means $|\vec{k}|$ in the following. The variables A, K, ϕ, and $\zeta_1(x)$ are supposed to be random, since the realistic sea surface shows statistical properties. Generally, an arbitrary statistic may be used in (2) and (3). At the first stage of our study, however, we assume for simplicity that A, K, and ϕ are deterministic. Then the average of σ is

$$\langle\sigma\rangle_h \sim \int_{-L}^{L}\int_{-L}^{L} dxdx' R(x,x') \left\langle e^{i\chi_z[\zeta_1(x)-\zeta_1(x')]}\right\rangle \tag{4}$$

where $R(x,x') = e^{i\chi_x(x-x')+i\chi_z A[\cos(Kx)-\cos(Kx')]}$.

According to [12] and [13], the average calculated for the assumption of normally distributed variables ζ_k results in

$$\left\langle \exp\left[i\sum_{k=1}^{n} q_k\zeta_k\right]\right\rangle = \exp\left\{-\frac{1}{2}\sum_{r,s=1}^{n}\mu_{rs}(\zeta_r,\zeta_s)q_r q_s\right\}, \tag{5}$$

with $n = 1, 2,\ q_{1,2} = \chi_z,\ \mu_{rs}(\zeta_r,\zeta_s) = \langle\zeta_r,\zeta_s\rangle$. Being expressed in terms of the rms-height of the small-scale roughness, $h^2 = \langle\zeta_1^2\rangle$ and the correlation function $C(u) = h^{-2}\langle\zeta_1(x)\zeta_1(x+u)\rangle$, where $u = x-x'$, the function μ_{rs} is given by $\mu_{rs} = -h^2C(u)$ at $r \neq s$ and by $\mu_{rs} = h^2$ at $r = s$. Then one obtains the following expression instead of (4):

$$\langle\sigma\rangle_h = e^{-(\chi_z h)^2}\int_{-L}^{L}\int_{-L}^{L} dxdx' R(x,x') e^{(\chi_z h)^2 C(u)}. \tag{6}$$

We restrict ourselves to the case of Gaussian statistics, so that the correlation function is given by $C(u) = \exp(-u^2/l^2)$ where l means correlation length.

Expanding the exponential term in the integral of (6) into a Taylor series, one yields

$$\langle\sigma\rangle_h = \sum_{m=0}^{\infty} \langle\sigma\rangle_h^m \tag{7}$$

where

$$\langle\sigma\rangle_h^m = e^{-(\chi_z h)^2}(\chi_z h)^{2m}(m!)^{-1} \int_{-L}^{L}\int_{-L}^{L} dx dx' R(x,x') e^{-u^2 m/l^2}. \tag{8}$$

For convenience of evaluating the integral in (8) at $m \geq 1$, we use relative coordinates $u = x - x'$, $v = x + x'$. On the other hand, coordinates x, x' seem to be more suitable than u, v for $m = 0$. Rewriting (8) in the new coordinates, one obtains

$$\langle\sigma\rangle_h^m = e^{-(\chi_z h)^2}(\chi_z h)^{2m}(m!)^{-1} \iint_{S_0} du dv\, T(u,v) e^{-u^2 m/l^2}. \tag{9}$$

Here $T(u,v) = e^{i\chi_x u - i2\chi_z A\sin(Ku/2)\sin(Kv/2-\delta)}$ with $\delta = KL - \phi$, S_0 means area over which the integration is carried out. This area is limited by $u \leq v \leq 4L - u$ at $0 \leq u \leq 2L$ and by $-u \leq v \leq 4L + u$ at $-2L \leq u \leq 0$.

Now the term in the expression for T, which shows nonlinear dependence on u, is expanded into a Taylor series. Applying the binomial series to the obtained expression leads to

$$T(u,v) = \sum_{r=0}^{\infty}(-1)^r (r!)^{-1}\left[\chi_z A \sin(Kv/2-\delta)\right]^r \sum_{s=0}^{r}(-1)^s C_r^s e^{i\frac{Ku}{2}(r-2s)+i\chi_x u} \tag{10}$$

where $C_r^s = r!/[s!(r-s)!]$ are the binomial coefficients. Substituting (10) into (9) and integrating over v, one obtains

$$\langle\sigma\rangle_h^m = e^{-(\chi_z h)^2}(\chi_z h)^{2m}(2m!)^{-1}\sum_{r=0}^{\infty}(-\chi_z A)^r (r!)^{-1}\sum_{s=0}^{\infty}(-1)^s C_r^s \sum_{j=1}^{3} b_j \Phi_j. \tag{11}$$

The coefficients b_j are given by $b_1 = C_{2r}^r 2^{-2r} KL$, $b_2 = (-1)^r 2^{2-r}$, $b_3 = (-1)^r 2^{1-r}$. The integrals Φ_j in (11) read

$$\Phi_1 = 2\int_0^{2L} \cos\left[\frac{Ku}{2}(r-2s) + \chi_x u\right](1 - u/2L) e^{-u^2 m/l^2} du, \tag{12a}$$

$$\Phi_2 = 2\sum_{t=0}^{r-1}(-1)^t C_{2r}^t \int_0^{2L} B^e(r,t,u)\cos\left[\frac{Ku}{2}(r-2s)\right] e^{-u^2 m/l^2} du, \quad (12b)$$

where r is an even number, $B^e(r,t,u) = \cos[2(r-t)\phi]\sin[(r-t)(2KL-Ku)]/(r-t)$,

$$\Phi_3 = 2\sum_{t=0}^{r}(-1)^t C_{2r+1}^t \int_0^{2L} B^0(r,t,u)\cos\left[\frac{Ku}{2}(r-2s)\right] e^{-u^2 m/l^2} du, \quad (12c)$$

where r is an odd number, $B^0(r,t,u) = \sin[2(r-t+1/2)\phi]\sin[(r-t+1/2)(2KL-Ku)]/(r-t+1/2)$.

The integration carried out in (12a)–(12c) results in analytical expressions for $\Phi_{1,2,3}$ which represent a superposition of error functions [14] of complex argument, $D_1^{\pm} = 2\alpha L - i(\beta \pm \gamma)/2\alpha$, $D_2^{\pm} = i(\beta \pm \gamma)/2\alpha$, $D_3^{\pm} = 2\alpha L + i(\beta \pm \gamma)/2\alpha$ where $\alpha = \sqrt{m}/l$, $\beta = \frac{K}{2}(r-s)\chi_x$, $\gamma = (r-k)K$. γ shows nonzero value only for Φ_3. An additional term, which contains no error function appears for Φ_2. These expressions are very cumbersome and will be omitted here since a simplified version of the obtained expressions will only be used for further considerations.

For a realistic sea surface illuminated by electromagnetic waves in the millimeter wave range, the conditions

$$L/l \gg 1, \quad (13a)$$

$$K/\chi_x \ll 1, \quad (13b)$$

$$\chi_x K l^2 \ll 1 \quad (13c)$$

usually hold. In particular, these conditions are satisfied if the correlation length is in the range of millimeters, the spatial wavelength in the range of meters, and the linear size of the illuminated area measures meters or tens of meters. Note that the inequality (13b) is satisfied at least if θ_i or θ_s is not very close to zero.

Using the above inequalities, first consider the zero-term in the sum over m given in (7). It can be expressed as

$$\langle\sigma\rangle_h^0 = E_0 E_0^* \quad (14)$$

where the asterisk denotes the complex conjugate. In (14), E_0 is the normalized electric field corresponding to the case that $\zeta_1 = 0$ (see (1) and (3)). It is given by

$$E_0 = \int_{-L}^{L} dx e^{-i\chi_x x - i\chi_z A\cos(Kx+\phi)}. \quad (15)$$

In the case that there is no small roughness ($kh = 0$), the terms with $m \geq 1$ take zero value, so that $\langle\sigma\rangle_h$ is given by (14), (15). This case corresponds to scattering from a periodic surface of finite size. To convert (15) into a series, the Taylor series expansion and the binomial series are again invoked. The result reads

$$E_0 = \frac{1}{K} e^{i\chi_x \phi/K} \sum_{r=0}^{\infty} \frac{(-1)^r}{r!} \left(\frac{i\chi_z A}{2}\right)^r \sum_{s=0}^{r} C_r^s U(r,s)[i(r-2s) - i\chi_x/K]^{-1} \tag{16}$$

with $U(r,s) = e^{i(KL+\phi)(r-2s)-i(KL+\phi)\chi_x/K} - e^{-i(KL-\phi)(r-2s)+i(KL-\phi)\chi_x/K}$. If condition (13b) is satisfied, one can simplify (16). Carrying out some algebraic manipulations, one obtains instead of (14) and (16)

$$\langle\sigma\rangle_h^0 \approx \left(\frac{2}{\chi_x}\right)^2 \sin^2[\chi_x L - \chi_z A \sin(KL)\sin\phi]. \tag{17}$$

The latter expression defines the cross section for a periodic surface of finite size provided that (13b) is satisfied.

Now we return to the terms with $m \neq 0$. Imposing (13a) leads to the possibility to use the asymptotic value of the error function [14] and then to omit the terms of order e^{-z^2} and z^{-1} where $z = L/l$ in the expressions obtained by integrating (12a)–(12c) over u. If condition (13b) is satisfied, the result of the latter simplification can approximately be transformed into a relation in which the series over s and t can be split. The series over s can then be summarized. The result shows a form $(e^{-x} - 1)^r$ where $x = \chi_x \chi_z A K l^2/4m$, provided that $kl \sim 1$ and $AK < 1$. The condition (13c) allows us to use the first two terms of the Taylor series for the latter exponent. This leads to the very important advantage that the powers of $\chi_x \chi_z AK/4\alpha^2 \sim 1$ where $\alpha = \sqrt{m}/l$ appears in the series over r instead of the powers of $\chi_z A/2$ which can be much larger than unity.

As a result, one obtains instead of (11) and (12)

$$\langle\sigma\rangle_h^m \approx 2\sqrt{\pi} L e^{-(\chi_z h)^2} (\chi_z h)^{2m} (\alpha m!)^{-1} e^{-\chi_x^2/4\alpha^2} \sum_{j=1}^{3} W_j \tag{18}$$

where

$$W_1 = J_0(i2G), \tag{19a}$$

$$W_2 = \frac{1}{KL} \sum_{r=0}^{\infty} \frac{(-1)^r}{(2r)!} G^{2r} \sum_{t=0}^{r-1} \frac{(-1)^t}{r-t} C_{2r}^t D^e(r,t), \tag{19b}$$

$$W_3 = \frac{1}{KL} \sum_{r=0}^{\infty} \frac{(-1)^{r+1}}{(2r+1)!} G^{2r+1} \sum_{t=0}^{r} \frac{(-1)^t}{r-t+1/2} C_{2r+1}^t D^0(r,t). \tag{19c}$$

Here $J_0(x)$ is the Bessel function of zeroth order, $G = \chi_x \chi_z AK/4\alpha^2$ with $\alpha = \sqrt{m}/l$,

$$D^e(r,t) = \sin[2(r-t)KL]\cos[2(r-t)\phi] \cdot \left\{ ch\left[\frac{(r-t)\chi_x K}{2\alpha^2}\right] - i\, erf(i\chi_x/2\alpha) sh\left[\frac{(r-t)\chi_x K}{2\alpha^2}\right]\right\},$$

$$D^0(r,t) = \sin[2(r-t+1/2)KL]\cos[2(r-t+1/2)\phi] \cdot \left\{ ch\left[\frac{(r-t+1/2)\chi_x K}{2\alpha^2}\right] - i\, erf(i\chi_x/2\alpha) sh\left[\frac{(r-t+1/2)\chi_x K}{2\alpha^2}\right]\right\}$$

where $erf(x)$ means the error function (see [14]).

As can be seen from the above consideration, the integral representation of the cross section given by (6) is converted into a series one given by (7), (17)–(19). Note that the series over m and t in (7), (19b), and (19c) shows fast convergence for the most part of the range of variation of the parameters corresponding to a realistic sea surface, at least if electromagnetic waves of millimeter wave range are applied. Although the solution given by (7), (17)–(19) looks more cumbersome than the integral representation of the solution given by (6), the structure of the obtained series is more convenient for analytical and numerical studies of the effect of parameters of both the surface and incident wave on the scattering cross section.

3. ANALYSIS

Consider the case of backscattering which is of most practical importance for remote sensing applications. In this case $\theta_s = -\theta_i$, so that $\chi_x = 2k\sin\theta_i$, $\chi_z = 2k\cos\theta_i$. Firstly suppose that there is no long wave (periodic component) in the random surface description, i.e., $A = 0$, $G = 0$, and that the linear size of the scattering area is so large that $KL \gg 1$. Then the cross section normalized by the factor L/k is given by

$$\langle\sigma\rangle_h = 2kle^{-(\chi_z h)^2} \sum_{m=1}^{\infty} \sqrt{\frac{\pi}{m}} \frac{(\chi_z h)^{2m}}{m!} e^{-(\chi_x l)^2/4m}. \tag{20}$$

The above result corresponds to the scattering cross section given in [9, 15]. It is known as the regular full-wave scattering cross section. Provided that all terms beyond the first one are small, relation (20) gives first-order perturbation results.

Now assume that the long periodic spatial structure has a small amplitude, i.e., $AK \ll 1$. If, moreover, the condition

$$G = \chi_x \chi_z l^2 AK/4m \ll 1 \tag{21}$$

is satisfied, the Bessel function in term W_1 given by (19a) can be estimated as

$$J_0(2iG) = \sum_{t=0}^{\infty} \frac{1}{(t!)^2} G^{2t} \approx 1. \tag{22}$$

The condition (21) introduces a ratio between the parameters of long waves and those of small-scale roughness, at which $\langle\sigma\rangle_h$ weakly depends on the amplitude of the long waves. Thus, if the parameter kl is increased, AK should sufficiently be decreased in order to satisfy (21).

Consider (19a)–(19c). Contrary to $W_1 \approx 1$, W_2 and W_3 contain parameters of both periodic and small-scale components. Thus the finite area effect depends on the small-scale roughness only due to these terms. It can be seen from (19b) and (19c), that the series over r contains the powers of G, starting either from the first one in the general case or from the second one in the case that $\phi = 0$. This means that the contribution of W_2 and W_3 is insignificant at least if (21) holds and $KL > 1$. In this case, one can use only the first terms of the series representation for W_2 and W_3. Then $W_2 = 0$ and $W_3 = PG\mathrm{sinc}(KL)$, where $P = \cos\phi[ch(\frac{\chi_x K}{4\alpha^2}) - i\, erf(\frac{i\chi_x}{2\alpha}) sh(\frac{\chi_x K}{4\alpha^2})]$, $\mathrm{sinc}\, x = \sin x/x$. As a result, we obtain the following formula for the normalized cross section:

$$\langle\sigma\rangle_h = \langle\sigma\rangle_h^0 + \sum_{m=1}^{\infty} \langle\sigma\rangle_h^m \tag{23}$$

where $\langle\sigma\rangle_h^0$ is given by (17) multiplied by k/L,

$$\langle\sigma\rangle_h^m = 2kle^{-(\chi_z h)^2} \sqrt{\frac{\pi}{m}} \frac{(\chi_z h)^{2m}}{m!} e^{-(\chi_z l)^2/4m} [1 + 2PG\mathrm{sinc}(KL)].$$

Consider the structure of the simplified expression for the scattering cross section (23). As mentioned above, the first term on the right-hand side of (23) only describes the diffraction effect on the periodical finite-size structure and does not depend on the random parameters of the surface. On the other hand, the second term in (23) is responsible for scattering by the randomly rough surface. It is seen that $\langle\sigma\rangle_h^m$ consists of two terms. The first of them is not connected with a long spatial wave. The second one contains the parameters of both the long spatial wave and the small-scale roughness. This term is proportional to G and is hence small compared to the first one. As can be seen, increasing the scattering area results in decreasing this term. Thus the effect of the long wave amplitude variation on the cross section is most pronounced for small sizes of the scattering area.

In the general case, if (21) is not satisfied, one should use the following expression for $\langle\sigma\rangle_h^m$ in (23)

$$\langle\sigma\rangle_h^m = 2kle^{-(\chi_z h)^2}\sqrt{\frac{\pi}{m}}\frac{(\chi_z h)^{2m}}{m!}e^{-(\chi_x l)^2/4m}\sum_{j=1}^{3}W_j.$$

If $G \sim 1$, the terms W_2 and W_3 are still vanishingly small at $KL \gg 1$ and hence responsible for the finite area effect only if KL is small enough, as is the zero-term which is proportional to (17). In the case of KL being small enough, $G(KL)^{-1}$ can be ~ 1 even though $G \ll 1$, so that one cannot consider W_2 and W_3 to be negligibly small in comparison with W_1 if just condition (21) is satisfied. If the inequality

$$(kl)^2 AK \sin 2\theta_i/(2mKL) \ll 1 \tag{24}$$

is not satisfied, one must take into account the contributions of the terms W_2 and W_3. This condition is necessary to provide the dependence of the effect of the parameters of small-scale roughness on the amplitude A, which does not occur in the framework of the above used approximations. Yet another effect which occurs if one takes into account these terms is the dependence of $\langle\sigma\rangle_h$ on the phase of the periodic surface (see (3), (19b), and (19c)).

Consider the first term W_1. Regarding the angular behaviour, the function G reaches its maximum at $\theta_i = \pi/4$. The larger kl and AK, the more pronounced is this maximum, and thus the stronger is the effect of G on $\langle\sigma\rangle_h^m$. Thus if (21) does not hold, one should expect that a maximum of $\langle\sigma\rangle_h$ appears except for the case that the zeroth term $\langle\sigma\rangle_h^0$ makes the dominant contribution to the cross section over the total range of angle variation.

Since $J_0(i2G)$ depends on m, it plays the role of weighting coefficients in the sum over m. Increasing m results in decreasing $J_0(i2G)$. Thus the contribution of the terms in the sum over m varies in favour of those with smaller m, as $|\theta_i - \pi/4|$ decreases. This occurs if $G \sim 1$ or if $G > 1$, i.e., when the condition

$$(kl)^2 AK \sin 2\theta_i/(2m) \sim 1 \tag{25}$$

is satisfied. One cannot split the effects of the periodic (long wave) and of the small-scale components if (25) is valid. The effect of the finite area becomes weaker in the middle-angle region. This is due to the decreasing contribution of $\langle\sigma\rangle_h^0$ to (7) and (23) which is caused by an increasing J_0 with G. As follows from (25), the amplitude A can exert a weak effect on the scattering at $kl \ll 1$, even though $AK \sim 1$. This result holds for arbitrary θ_i.

Thus we have carried out a qualitative analysis of the obtained series-type solution in the backscattering case. As a result, we have obtained the conditions at which the finite-area effect is more pronounced, and those for which one can expect that the effect of one or the other parameter should be insignificant. Now let us validate the developed theory by comparing it to numerical results.

4. SIMULATION RESULTS

We will first consider how the variations of random parameters which are related to the different ranges of the roughness spectrum, influence the intensity of the scattered electromagnetic waves. Consider the case that the large-scale roughness is deterministic. Then the model of the sea surface consists of a cosine wave with wavelength Λ which is much larger than the wavelength of the electromagnetic wave λ, superposed to a small-scale roughness whose rms-height h and correlation length l satisfy the conditions $Kh \ll 1$ and $Kl \ll 1$. Note that according to [16], the parameters of the random surface and the surface length L, at which the averaging may be used, must satisfy the conditions $40h \geq L$ and $200l \geq L$.

The formulae (7), (17)–(19) have been applied for calculations, in which the cross section has been normalized by the term $2\sqrt{\pi}L/\chi_z$. In Figs. 1–4, we show the angular behaviour of the radar scattering cross section for different parameters of the random surface. The backscattered signals are studied because this case usually represents the practical situation.

Fig. 1 shows plots for different rms-heights while the correlation length is kept constant, for the case that the size of the illuminated surface is almost the same as the spatial wavelength of the long waves. The smaller the h-value, the narrower is the roughness spectrum. This narrowing leads to an increasing contribution of diffraction from the periodically finite surface to the scattering process. As is shown in Fig. 1(a), which corresponds to the smaller kh-value, a diffraction effect occurs in the angle range of 45 to 80 degrees. An increase of the rms-height results in shortening this angle range, at which diffraction is dominant (see Figs. 1(a)–(c)). The diffraction effect dependence on the size of the illuminated area can be seen from comparing the results of Figs. 1 and 2. Figure 2 shows the angular dependence of the cross section for the same surface parameters as in Fig. 1 except the illuminated area size, which is almost ten times as large as the spatial wavelength of the long waves. One can see that increasing the scattering area leads to decreasing the angle range, which corresponds to the dominant contribution of diffraction. In the considered case,

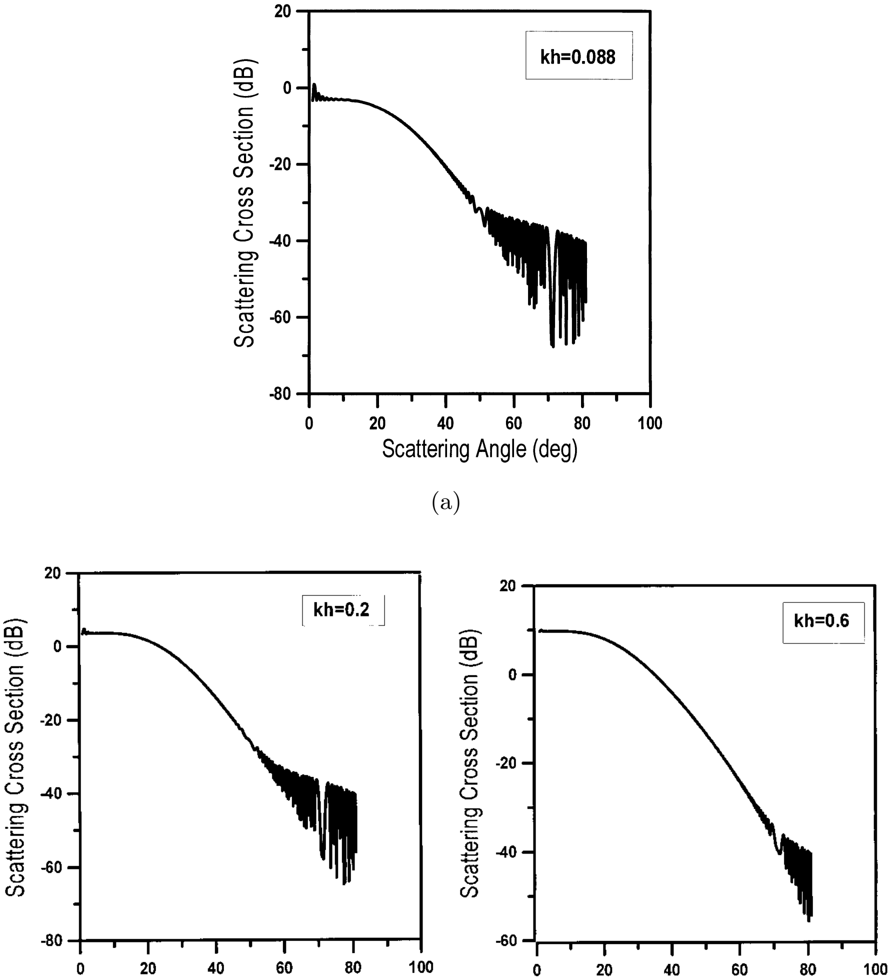

Figure 1. Angular behaviour of the scattering cross section for different rms-heights and constant value of the correlation length $l = 2.7/k$. The illuminated area is small: $L = 6/K$; the amplitude of the large surface wave is $A = 0.3/K$; the phase of this wave is $\phi = \pi/20$; the relation between the wave numbers of the large surface and electromagnetic waves is $K/k = 3 \cdot 10^{-3}$; a) $h = 0.088/k$, b) $h = 0.2/k$, c) $h = 0.6/k$.

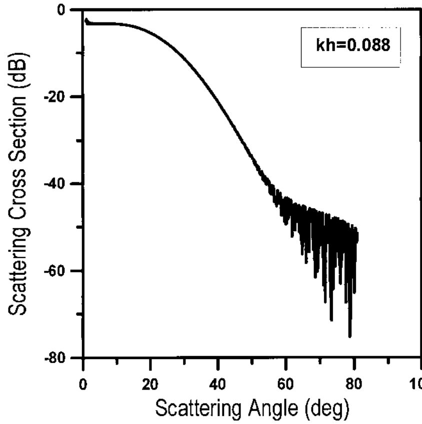

(a)

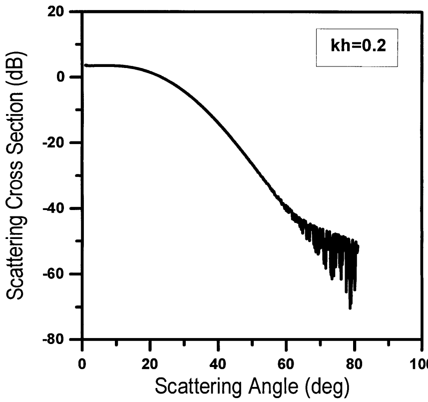

(b)

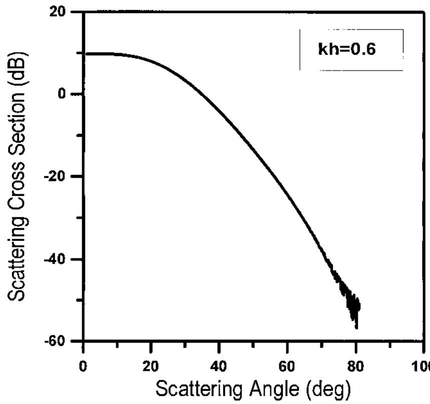

(c)

Figure 2. Angular behaviour of the scattering cross section for different rms-heights and constant value of the correlation length $l = 2.7/k$. The illuminated area is moderate: $L = 60/K$; the amplitude of the large surface wave is $A = 0.3/K$; the phase of this wave is $\phi = \pi/20$; the relation between the wave numbers of the large surface and electromagnetic waves is $K/k = 3 \cdot 10^{-3}$; a) $h = 0.088/k$, b) $h = 0.2/k$, c) $h = 0.6/k$.

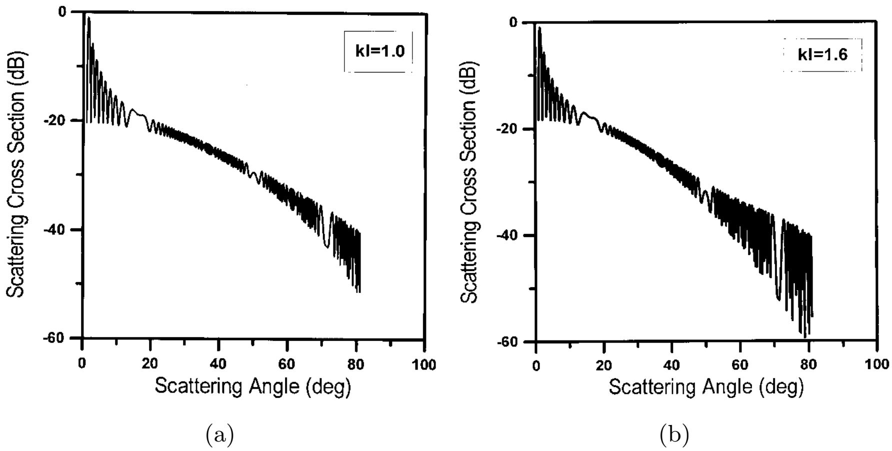

Figure 3. Angular behaviour of the scattering cross section for different correlation lengths l and constant value of the rms-height $h = 0.02/k$. The illuminated area is small: $L = 6/K$; the amplitude of the large surface wave is $A = 0.3/K$; the phase of this wave is $\phi = \pi/20$; the relation between the wave numbers of the large surface and electromagnetic waves is $K/k = 3 \cdot 10^{-3}$; a) $l = 1/k$, b) $l = 1.6/k$.

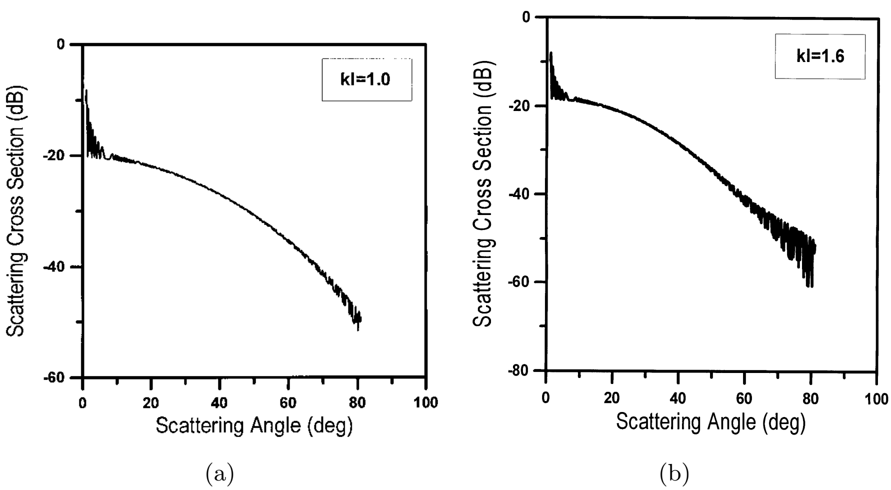

Figure 4. Angular behaviour of the scattering cross section for different correlation lengths l and constant value of the rms-height $h = 0.02/k$. The illuminated area is moderate: $L = 60/K$; the amplitude of the large surface wave is $A = 0.3/K$; the phase of this wave is $\phi = \pi/20$; the relation between the wave numbers of the large surface and electromagnetic waves is $K/k = 3 \cdot 10^{-3}$; a) $l = 1/k$, b) $l = 1.6/k$.

the factor $(kl)^2AK/(2m)$ at $m = 1$ takes the value 1.09, so that (25) is satisfied, and hence the long wave amplitude affects the scattering from small-scale roughness substantially.

Now consider how the variation of the correlation length affects the scattering process. If the value of the rms-height is sufficiently small like that one in the curves of Figs. 3 and 4, then the effect of the diffraction strongly manifests itself in the scattering process. Since an increase of the value of the correlation length at constant rms-height corresponds to narrowing the roughness spectrum of the small-scale roughness, one should expect an increasing contribution of the diffraction effect. Note that the presence of oil films on sea surface can lead to similar phenomena. As can be seen from Figs. 3 and 4, a decreasing influence of the small-scale roughness or, correspondingly, an increasing correlation length leads to a redistribution of the diffraction part in the angular behaviour of the scattered intensity (compare Figs. 3(a), 3(b), 4(a), and 4(b)). The increase of the correlation length results in an insignificant decrease of the diffraction effect at the middle-angle range. The opposite trend is observed at large angles. In this case, an increase of kl results in a substantial increase of the contribution of the diffraction effect. One can observe a larger value of the cross section for smaller kl, which is caused by increasing scattering from the small-scale roughness due to an increased slope. A comparison of the curves with the same roughness parameters but with two different lengths of the scattering surface (see Figs. 3 and 4) indicates that an increase of the size of the scattering area causes the diffraction effect to decrease, so that the scattering from the small-scale roughness is prevalent for the most part of the angle range. In the considered case, (25) is not yet satisfied, but (21) is already not satisfied. Thus, the long wave amplitude exerts no substantial effect on the scattering from the small-scale roughness. The effect of the finite size of the illuminated area manifests itself only through the diffraction term $\langle\sigma\rangle_h^0$.

To study the influence of the different scattering mechanisms on the scattering cross section, its angular behaviour has also been computed for different rms-heights and correlation lengths which have been changed simultaneously in such a manner that the slope angle of the small-scale roughness has been kept constant. Fig. 5(a) depicts the scattering cross section when h and l have so small values that diffraction becomes the major scattering mechanism over the whole range of angle variation. In this case, one can observe that the level of the scattered intensity is higher in the case of smaller KL. The influence of both KL and AK for larger values of h and l appears to be negligible for most part of the angle range, as is shown in Fig.

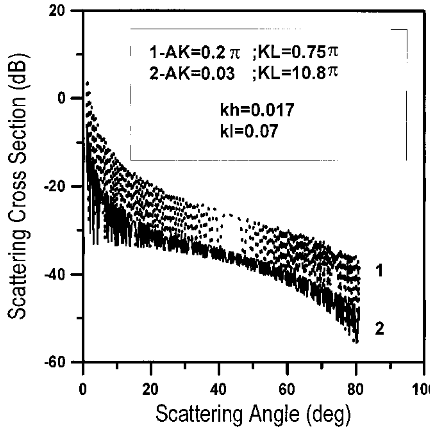

(a)

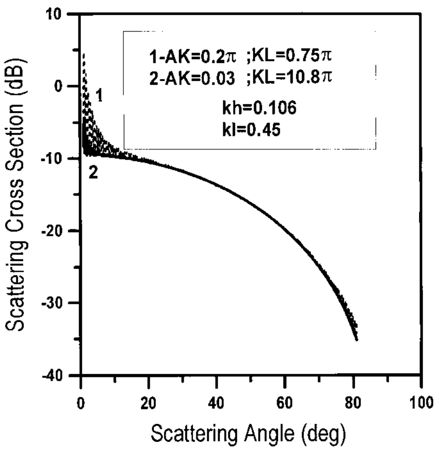

(b)

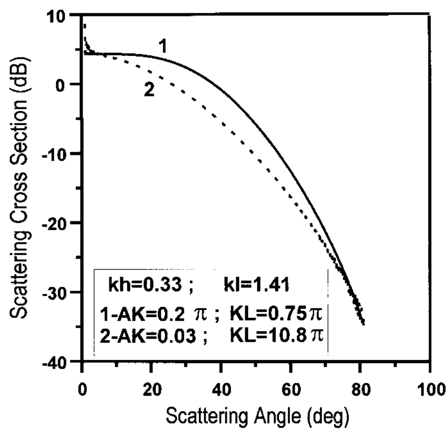

(c)

Figure 5. Role of an illuminated area and an amplitude of the long surface wave. Scattering cross section as a function of the incidence angle for constant slope angle of the small-scale roughness. The phase of the large surface wave is $\pi/4$; the relation between the wave numbers of the surface and electromagnetic waves is $3 \cdot 10^{-3}$.

a) The rms height is $0.017/k$ the correlation length is $0.07/k$;

b) the rms height is $0.106/k$, the correlation length is $0.45/k$;

c) the rms height is $0.331/k$, the correlation length is $1.41/k$.

5(b). This result can be explained by noting that scattering from the small-scale roughness plays a major role. In line with (21) and (25), the long wave amplitude does not affect the above scattering mechanism in the considered case. A further increase of h and l will raise the influence of the large-scale spatial wave on the scattering as is demonstrated in Fig. 5(c). It can be observed that an increase of the large wave amplitude results in an increase of the scattering level due to improving the satisfying condition (25). The variation of the area size just weakly affects the scattering in this case.

As next step of our study, we assume that the amplitude of the large wave A is a random value, hence we apply ensemble averaging. The results obtained above for the case without averaging over A can be used to estimate the range of variation of the surface parameters, for which the averaging should be carried out. In particular, it can be seen from (25) that the larger AK and kl, the larger is the expected difference between the averaged and the non-averaged cross sections. This effect should be most pronounced at intermediate angles. On the other hand, if (25) is satisfied and KL is large enough, an averaging effect is not expected for those parameters, for which the terms with $m \geq 1$ constitute the dominant contribution to (7) and (23). The other expected effect of averaging is caused by the appearance of term A in the diffraction term (17). In this case, the oscillations of $\langle\sigma\rangle_h$, which appear for the non-averaged cross section should be damped. In the frame of the above consideration, this effect should be pronounced at small and large angles.

Now generate a series of normally distributed variables. It is given by

$$R'_i = \sqrt{2\ln(1/V_i)}\cos(2\pi V_{i-1}), \tag{26a}$$

$$R''_i = \sqrt{2\ln(1/V_i)}\sin(2\pi V_{i-1}) \tag{26b}$$

with $V_{i+1} = FRAC(k_t V_i)$ where $FRAC(x)$ means the fractional part of the number, $k_t = 8t \pm 3,\ t$ is an odd integer, $i = 1, 2, \ldots$. The initial value V_0 is an arbitrary number satisfying the inequality $0 < V_0 < 1$. Also $R_{2i-1} = R'_i,\ R_{2i} = R''_i$. As a result, a conjugate pair of numbers with zero mean value, $\overline{R} = 0$, and rms-deviation $\langle a^2\rangle = 1$ is obtained for each i. To obtain a series with $\overline{R} \neq 0$, $\langle a^2\rangle \neq 1$, the building law

$$r_{i+1} = \overline{R} + R_{i+1}\left\langle a^2\right\rangle \tag{27}$$

is used. As soon as the numbers r_i are determined, the calculation of the scattering cross section can be carried out by using (7), (17), (18),

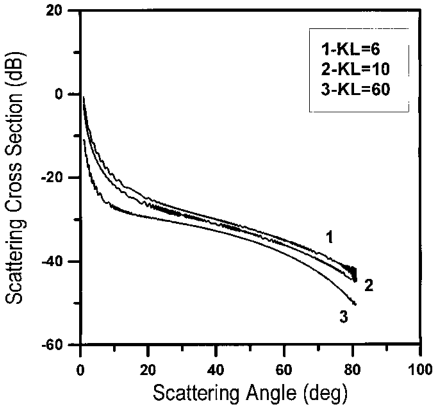

(a)

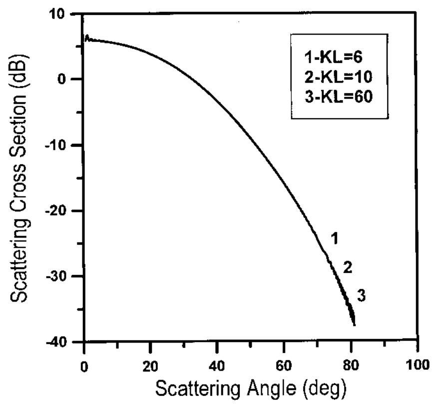

(b)

Figure 6. Role of the scattering area size for two-scale rough surface with different parameters of small-scale roughness. The parameters of the large surface wave are: $A = 0.3/K$, $\phi = \pi/20$, $K/k = 3 \cdot 10^{-3}$; a) $h = 0.02/k$, $l = 0.12/k$; b) $h = 0.4/k$, $l = 1.6/k$.

(19), and supposing that $A = r_i$. Finally, we average the obtained results. The variable $\langle\sigma\rangle = \langle\langle\sigma\rangle_h\rangle_A$ is referred to as the scattering cross section, since the cross sections obtained without averaging with respect to the amplitudes of the long waves are not considered any longer. The normalization factor $2\sqrt{\pi}L/\chi_z$ is used as in the case that no averaging was applied.

Consider now the two-scale rough surface with small roughness as has been described above, and with superposed large roughness. A presentation of the surface by cosine waves with random amplitudes is a mean to take the surface inhomogeneity into account. Here we provide ensemble averaging for the large-scale component supposing that the wave vector and phase are deterministic. For all following results, the averaging is carried out for $N = 60$ curves with a rms-deviation equal to 0.15.

Fig. 6 presents the results for small (a) and moderate (b) values of the small-scale roughness parameters. The curves 1, 2, 3 correspond to scattering surfaces with lengths $6/K$, $10/K$, $60/K$, respectively. The shorter the length of the scattering surface, the stronger is the backscattered signal which occurs mainly because of the influence of diffraction. In line with this, the scattering for a length $L = 6/K$ (curve 1) is stronger than for $L = 60/K$ (curve 3) as can be seen from Fig. 6(a). If the scattering due to the small-scale roughness is dominant, the scattering area has no effect on the values of the radar cross section,

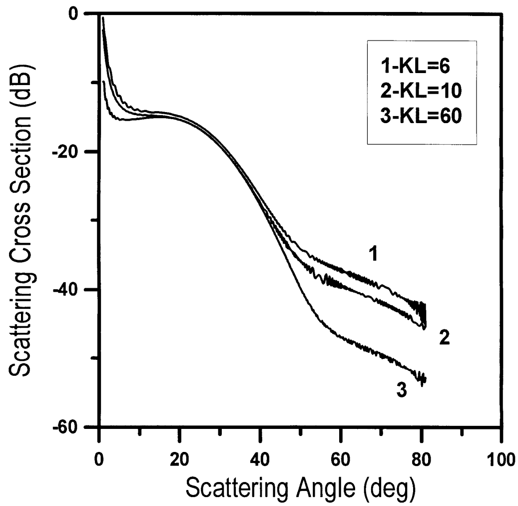

Figure 7. Role of the scattering area size for two-scale rough surface with constant correlation length which has been set equal to $2.7/k$ and different rms-height which is equal to $0.02/k$. The parameters of the large surface wave are: $A = 0.3/K$, $\phi = \pi/20$, $K/k = 3 \cdot 10^{-3}$.

as one can see in Fig. 6(b) (all three curves merge together). The latter corresponds to the case that the term $\langle\sigma\rangle_h^0$ can be omitted, as well as the terms W_2 and W_3. (Note that in Fig. 6 and further A means a mean value of the long wave amplitude). Thus the effect of the scattering area size can manifest itself for the surface covered by an oil film.

The results in Fig. 7 belong to a small-scale roughness with the same rms-height as in Fig. 6(a), and sufficiently large correlation length. Again as in Fig. 1, the contribution to the scattered signal caused by diffraction is most significant at large angles, because in this case the effect of the area size is most pronounced. However, if the small-scale roughness parameters are sufficiently small, the influence of the long wave will be extended over the whole angle range. The decrease of the effect of KL on the cross section at angles of 15 to 40 degrees is caused by the increasing contribution of term W_1 given by (19a) to the whole cross section which occurs due to an increasing G (see (21)).

The results in Fig. 8 show the scattering for several values of the rms-height when the correlation length is equal to $2.7/k$. The linear size of the scattering surface is equal to $L = 10/K$ in Fig. 8(a)

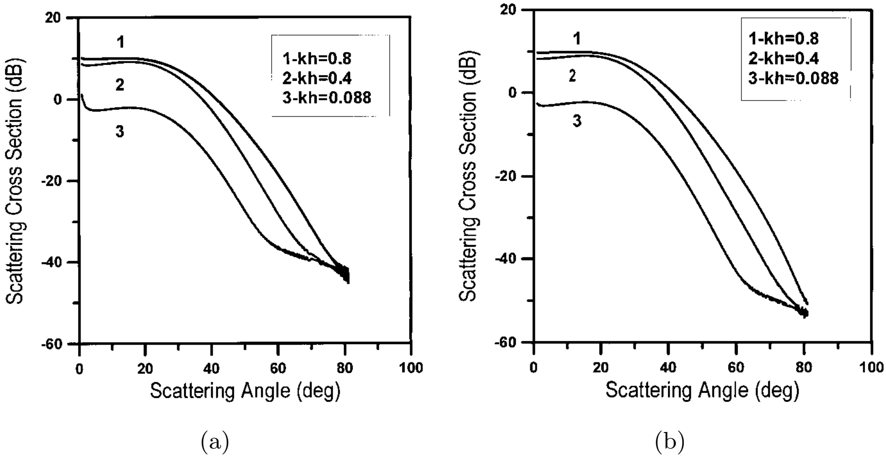

Figure 8. Effect of the rms-height on the scattering cross section for different size of the scattering area (correlation length $l = 2.7/k$). The parameters of the large surface wave are: $A = 0.3/K$, $\phi = \pi/20$, $K/k = 3 \cdot 10^{-3}$; a) $L = 10/K$; b) $L = 60/K$.

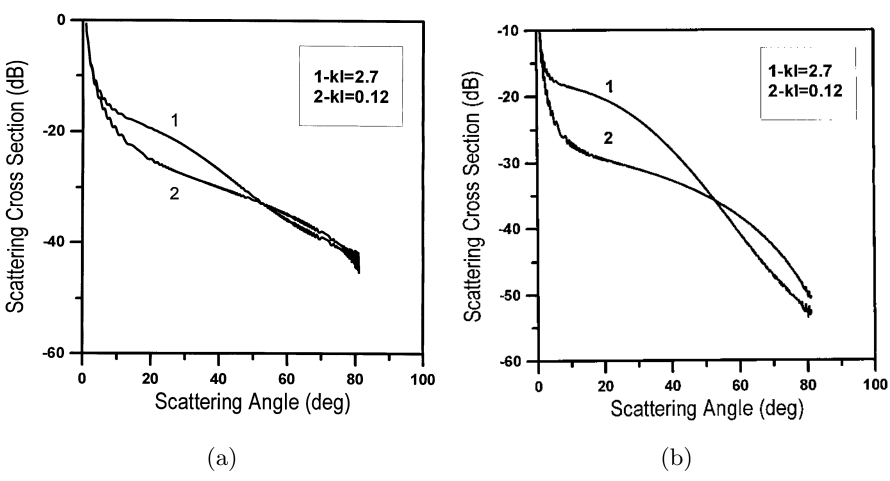

Figure 9. Effect of the correlation length on the scattering cross section for different size of the scattering area (rms-height $h = 0.02/k$). The parameters of the large surface wave are: $A = 0.3/K$, $\phi = \pi/20$, $K/k = 3 \cdot 10^{-3}$; a) $K = 10/L$; b) $L = 60/L$.

and to $60/K$ in Fig. 8(b). An increase of the scattered signal with the rms-height increased is not observed at angles close to 80 degrees, provided that kh is small enough, what is due to the dominant effect of diffraction. In the other cases, the effect of kh on the cross section is usually quite pronounced. An increase of the scattering area leads to a substantial decrease of the cross section if the angle is larger than 60 degrees.

Lastly we consider the case that the correlation length is varied while the rms-height is constant at a small value which may correspond to the surface with an oil slick. Then the small-scale roughness spectrum is sufficiently narrow and the spectral strength in the angular range close to horizontal incidence is low. This phenomenon causes reduced backscattering from small-scale roughness. Hence the scattering cross section in the angular range of 50 to 90 degrees mainly depends on the diffraction effect. The shorter the linear size of the scattering area, the stronger is the contribution of diffraction and the larger is the cross section value, as is shown in Figs. 9(a) and 9(b).

5. CONCLUSIONS

To summarise, let us discuss the main features of this study from the point of view of oil slick determination by using SAR images. According to [4], oil films on sea lead to a suppression of backscattering over all ranges of the surface wave spectrum. However, to explain the backscattering reduction due to oil films it is often suggested that only a Bragg resonance process (i.e., short surface waves) is responsible for the scattering of electromagnetic waves, while non-linear wave-wave interaction transfers energy from long waves to an energy sink in the short-wave region.

As can be seen from the above study, long surface waves can directly suppress a backscattered signal from oil films. However, this decrease of the scattering which is observed for moderate values of the parameters of small-scale roughness, is sufficiently low if the small-scale roughness shows small values.

In general, the scattering signal consists of three parts: the diffraction caused by the finite size of the scattering area, the scattering from small-scale roughness, and the scattering from large-scale surface waves. All these factors can affect the value of the scattering cross section because of various relations existing between them. If the parameters of the small-scale roughness are sufficiently small, the diffraction plays a major role in backscattering. For such parameters of small-scale roughness, the amplitude of the large-scale roughness does not affect the scattering intensity as has been shown. This phenomenon leads to a level of the scattering cross section which depends on area size. The larger the size, the lower is the value of scattering. Hence in practice, SAR images of oil slicks obtained for a smaller illuminated area can show a higher level of response compared to those from a larger area even if the roughness shows the same values. As a result, the contrast between two backscattered signals, which correspond to the surfaces with and without oil slicks, while the large wave parameters are kept constant, may also depend on the area size.

On the other hand, it is also possible to observe the opposite phenomenon that the level of response is decreased as a result of a decrease in the amplitude of the long surface wave. In spite of the fact that this feature is observed for essentially larger parameters of small-scale roughness, the difference in contrast between two backscattered signals, which correspond to two different amplitudes of long waves, can be the same as the contrast for the case that the small-scale roughness parameters are smoothed due to the slick effect. In this case, one should expect just a very weak dependence on the scattering area size.

Hence a possible method for distinguishing between these mechanisms of the lowering of the level response is to study the influence of a finite size of the scattering area. Indeed, in order to determine what part of the roughness spectrum (short or long waves) is responsible for the decrease in scattering, one should compare the level of response from oil slicks for different size of the illuminated area.

REFERENCES

1. Solberg, S., G. Stowik, R. Solberg, and E. Volden, "Automatic detection of oil spills in ERS SAR images," *IEEE Trans. Geosci. Rem. Sens.,* Vol. GE-37, 1916–1925, 1999.
2. Alpers, W. and H. Huhnerfuss, "The damping of ocean waves by surface films: A new look at an old problem," *J. Geophys. Res.,* Vol. 94(C), 6251–6265, 1989.
3. Fiscella, B., P. P. Lombardini, and P. Trivera, "The impact of higher order Bragg terms on radar sea return," *Nuovo Cimento,* Vol. 8C, 118–124, 1982.
4. Maclin, J. T., "The imaging of oil slicks by synthetic-aperture radar," *GEC Journal of Research,* Vol. 10, 19–28, 1992.
5. Singh, K. P., A. L. Gray, R. K. Hawkins, and R. A. O'Neil, "The influence of surface oil on C- and Ku-band ocean backscatter," *IEEE Trans. Geosci. Rem. Sens.,* Vol. GE-24, 738–744, 1986.
6. Tatarskii, V. I. and S. F. Clifford, "On the theory of Δk radar

observations of ocean surface waves," *IEEE Trans. Antennas Propagat.,* Vol. AP-43, 843–850, 1995.

7. Ishimaru, A., *Wave Propagation and Scattering in Random Media,* Academic Press, New York, 1978.
8. Brown, G. S., "Backscattering from a Gaussian distributed perfectly conducting rough surface," *IEEE Trans. Antennas Propagat.,* Vol. AP-26, 472–482, 1978.
9. Collin, R. E., "Electromagnetic scattering from perfectly conducting rough surface (A new full wave method)," *IEEE Trans. Antennas Propagat.,* Vol. AP-40, 1466-1477, 1992.
10. Stratton, J. A., *Electromagnetic Theory,* McGraw-Hill, New York, 1941.
11. Holiday, D., L. L. DeRaad, Jr., and G. J. St-Cyr, "New equations for electromagnetic scattering by small perturbations of a perfectly conducting surface," *IEEE Trans. Antennas Propagat.,* Vol. AP-46, 1427–1432, 1998.
12. Rice, S., "Mathematical analysis of random noise," *Noise and Stochastic Processes,* N. Wax (Ed.), 182, Dover Publ., Inc., New York, 1954.
13. Lynch, P. J., "Curvature corrections to rough surface scattering at high frequencies," *J. Acoust. Soc. Am.,* Vol. 47, 804–815, 1970.
14. Abramovitz, M. and I. A. Stegun (Eds.), *Handbook of Mathematical Functions,* National Bureau of Standards, Appl. Math. Series-55, 1964.
15. Bahar, E., "Full wave analysis for rough surface diffuse, incoherent radar cross sections with height-slope correlation included," *IEEE Trans. Antennas Propagat.,* Vol. AP-39, 1293–1304, 1991.
16. Yisok, O. and C. K. Young, "Condition for precise measurement of soil surface roughness," *IEEE Trans. Geosci. Rem. Sens.,* Vol. GE-36, 691–695, 1998.